SHAKING TABLE TEST USING MULTIPURPOSE TEST BED

Toru Takeuchi[1], Kazuhiko Kasai[2], Mitsumasa Midorikawa[3], Yuichi Matsuoka[4], Takeshi Asakawa[5], Isao Kubodera[6], Yuji Kurokawa[6], Shoichi Kishiki[7] and Hirotaka Ando[8]

[1] Associate Professor Tokyo Institute of Technology, Japan
[2] Professor, Structural Engineering Research Center, Tokyo Institute of Technology, Japan
[3] Professor, Hokkaido University, Japan
[4] Nat. Res. Inst. for Earth Science and Disaster Prevention, Japan
[5] Nikken Sekkei Co., Ltd. Japan
[6] General Manager, Tomoe Corporation. Japan
[7] Assistant Professor, Tokyo Institute of Technology, Japan
[8] Graduate student, Tokyo Institute of Technology, Japan
ttoru@arch.titech.ac.jp, kasai@serc.titech.ac.jp, midorim@eng.hokudai.ac.jp, pinehill@bosai.go.jp, asakawa@nikken.co.jp, i_kubodera@tomoegiken.co.jp, kurokawa@tomoegiken.co.jp, , kishiki@serc.titech.ac.jp, ando3@mail.arch.titech.ac.jp

ABSTRACT :

This paper describes a multipurpose setup system called “test bed” for large shaking table tests. The test bed comprises multi-story box-trusses with concrete mass of inertia supported by linear slider bearings in each layer. It supports its own weight, and provides a horizontal inertia force to the specimen frame when it is connected each other and placed on the shaking table. In this paper, shaking table tests with a single-story sample frame with beam-end dampers are conducted. The test results are compared with the analytical results and the performances of the setup system are discussed.

KEYWORDS: Steel Structure, Shaking Table Test, Hysteretic Damper, Inertial Mass, Test Bed

1. INTRODUCTION

The E-Defense shake table facility, the world’s largest earthquake simulator, is being utilized for a major research project on steel buildings in Japan. E-Defense can shake a large specimen having a completely three-dimensional configuration. However, since the cost of such a specimen can be very high, testing a part of the specimen such as the plane frame of a building would be much more economical and would still yield meaningful data. Such test methods would also enable parametric studies requiring multiple specimens. Accordingly, the authors are currently constructing a so-called “test bed” having a multipurpose inertial mass system (Takeuchi, Kasai, et. al. 2007, 2008). This test bed will be utilized for the aforementioned study on innovative methods, involving researchers from both the US and Japan, as part of the NEES/E-Defense Collaboration Research Program.
The proposed test bed system is shown in Figure 1. One unit of the test bed comprises steel truss boxes with a plan of 6 m × 4.5 m and a height of 2.7 m. Each unit comprises a concrete slab with dimensions of 3000 mm × 4000 mm and a mass of 30 metric tons. In the case of unidirectional movement, one unit of the test bed is supported by two unidirectional linear sliders and two bidirectional linear sliders. If additional horizontal stiffness is required, rubber bearings can be substituted for linear sliders. The inertial forces are transferred to the test frame through load-cell units that can automatically measure the shear forces introduced in each floor. Further, the story drift between each floor is measured by LVDTs placed between each layer of units.
In this study, two test bed units are constructed, and several types of trial tests using plane steel frames are conducted. The dynamic characteristics and response of the system, including the smoothness of the linear slider and the equivalent damping ratio of the system are evaluated. Further, the performance and accuracy of the load-cell units and story-drift measurement system are confirmed.

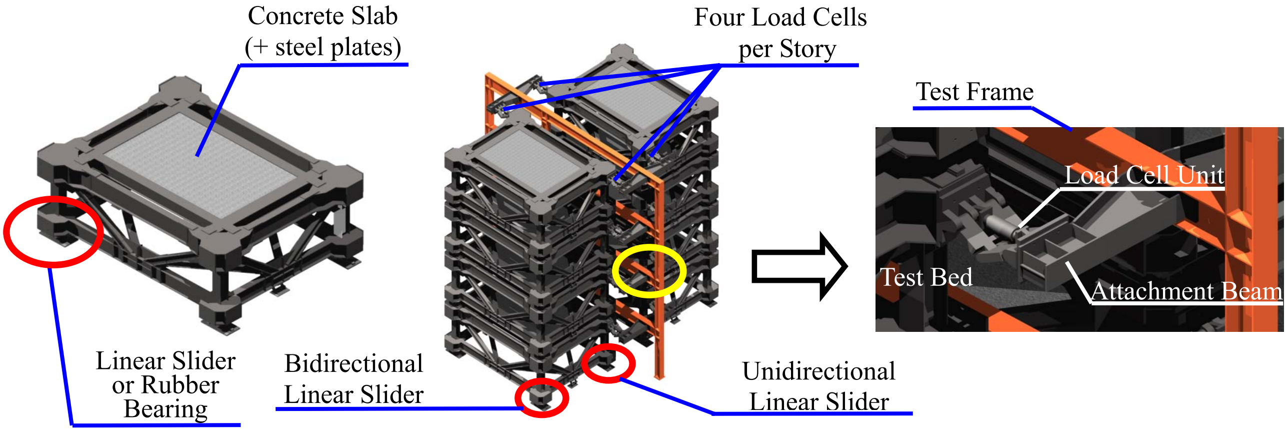

Figure 1 Test bed set-up for unidirectional shaking table tests

2. DESIGN OF THE TEST FRAME

The plane frame used in these tests comprises a passive response control structure system developed for medium height buildings. Figure 2 shows the elevation of a four-story office building frame with two spans. The beams with the longer span are rigidly connected to the columns, while the beams in the core part are connected to the columns by "beam-end dampers" (Kishiki et. al. 2006), as shown in Figure 2. This connection system comprises an elastic split-tee at the top flange and a replaceable plastic split-tee at the bottom flange of the beam. With the concrete floor slab, the center of rotation of the beam ends stays at the level of the elastic split-tee, and the plastic split-tee functions as a plastic damper, dissipating seismic energy. The plastic split-tee has a "dog-bone" shaped plastic area and it is restrained from buckling by the additional restrainer and the lower flange of the beam. In this system, the seismic energy input into the building is dissipated by the plastic split-tees; these can be replaced after they are damaged.

A cyclic test and fatigue test have been previously conducted for this system, and their basic characteristics have been confirmed.

The setup of the shake table test using the test bed system is shown in Figure 3, and the test frame using beam-end dampers is shown in Figure 4. The test frame is reduced to 70% scale. The detailed shapes of the elastic split-tee and plastic split-tee are shown in Figure 5. The elastic area of the plastic split-tee has two levels of hunch in order to measure the axial force of the damper using the strain gauges.

The single-story test frame was designed by referring to the response of the four-story building, as shown in Figure 6. The natural period of this four-story building is approximately 0.6 sec, while that of the test frame is 0.36 sec under elastic conditions. Accordingly, the time-scale of the earthquake input is reduced by half in order to model the response of the four-story building.

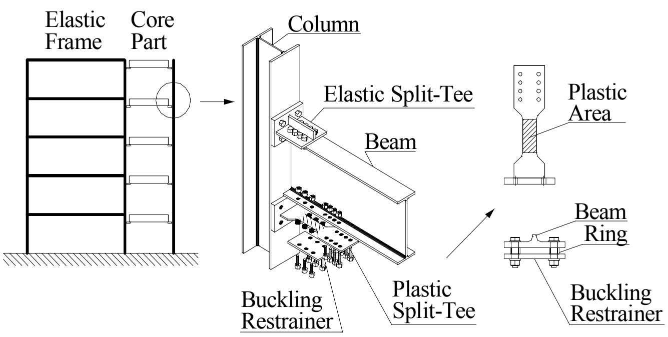

Figure 2 Beam-End Dampers System

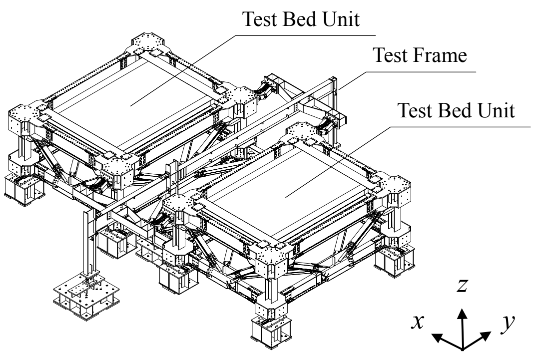

Figure 3 Test Set-up of Single Story Frame

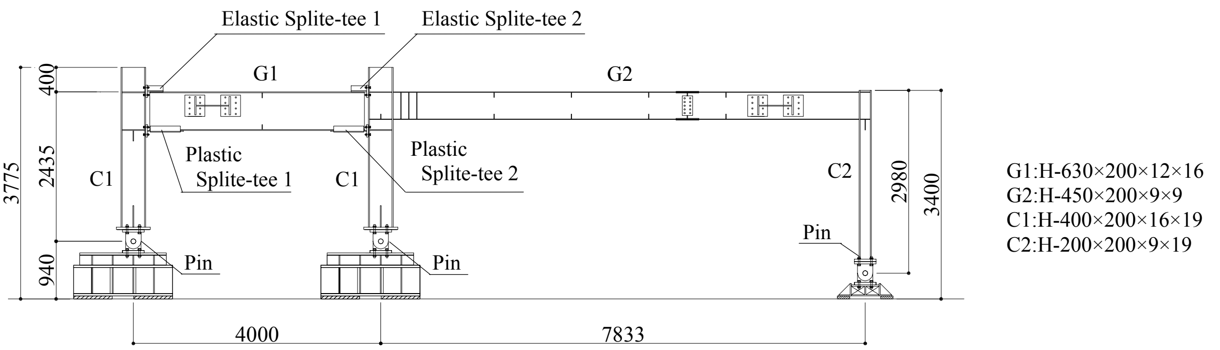

Figure 4 Test Frame Diagram

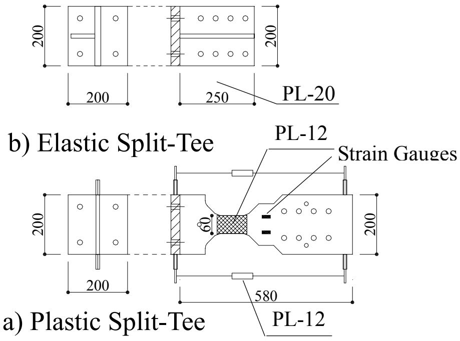

Figure 5 Beam End Damper

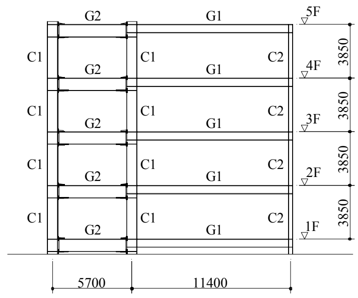

CODE	DIMENSION	STEEL PRODUCT
C1	H-700×300×19×25	SS400
C2	H-300×300×12×29	SS400
G1	H-600×300×12×29	SS400
G2	H-900×200×16×22	SS400
ST	PL-16~22×93	LY225

Figure 6 4-story Model Frame

The results of the time-history analyses for the response of a prototype four-story building and single-story test frame are compared in Figure 7. In this figure, the maximum acceleration responses of these models are generally found to be in agreement, and the designed test frame is considered to suitably simulate a real-sized four-story building. The shear force–story drift relationship in the test frame is shown in Figure 8. This figure shows that the plastic split-tees begin yielding at a story drift of approximately 6 mm (0.25% angle), and the test frame begins yielding at a story drift of 40 mm (1.8% angle).

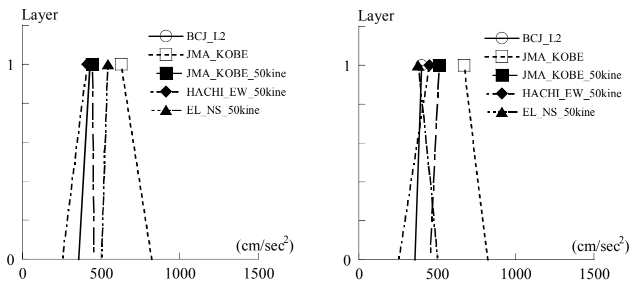

a) 4-Story Model b) Test Frame
Figure 7 Maximum Acceleration Response

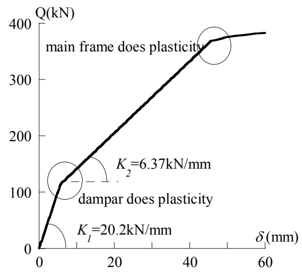

Figure 8 Shear Force–Story Drift Relationship

Next, the fracture point of the plastic split-tees at the beam end dampers is evaluated. The equation for evaluating the cumulative deformation capacity for buckling restrained braces has been proposed by Takeuchi and Ida (2008), and it is given as follows.

$$\chi(\%) = \frac{1}{\alpha_s / 35 + (1-\alpha_s)(\varepsilon_{ph}^{(1+m_2)} / (C_2/2))^{1/-m_2}} \quad (1)$$

χ : cumulative plastic strain
ε_{ph} : averaged plastic strain amplitude
α_s : skeleton hysteresis ratio

C_2 and m_2 are values obtained from the fatigue curve of the member, and this equation shows that the cumulative plastic strain of buckling restrained braces can be calculated from ε_{ph} and α_s. For a plastic split-tee, $C_2 = 43.9$ and $m_2 = -0.57$ have been obtained by Takeuchi and Shirabe (2006) as follows.

$$\chi(\%) = \frac{1}{\alpha_s / 35 + (1-\alpha_s)(\varepsilon_{ph}^{0.754} / 903)} \tag{2}$$

This equation can be used to obtain N_{seis}, the number of earthquakes until a fracture occurs. From the above method, it is expected that the plastic split-tees will fracture at third BCJ-L2 wave and the first JMA-KOBE wave.

3. SHAKING TABLE TEST

3.1. ELASTIC SHAKING TEST

First, the white noise test with frequencies ranging from 0.1 to 30 Hz is performed with a goal of A_{max}=100 cm/sec^2 in each direction to confirm the natural period of the system. The obtained acceleration transfer function is shown in Figure 9. This result shows that the natural frequency of the test frame along the Y-direction is 3.0 Hz; this is in agreement with the design value. From this frequency, the stiffness of the system is evaluated, as shown in Figure 10.

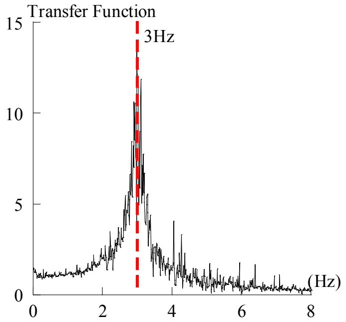

Figure 9 Transfer Function in Y-Direction

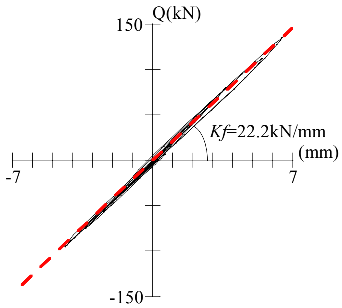

Figure 10 Shear Force-Displacement Relationships

Then, the sine wave test is performed to confirm the damping performance of the system. Three sine waves with a frequency of 5.0 Hz and amplitude of A_{max}=150 cm/sec^2 were input. The time-history of the displacement along the Y-direction is shown in Figure 11. This figure shows that the displacement of the test beds and the test frame is almost consistent. The amplitude ratio d is estimated from this figure, and the equivalent damping constant h is derived from Eq. (3).

$$h = \left(\frac{\ln d}{2\pi}\right) \Bigg/ \sqrt{1 + \left(\frac{\ln d}{2\pi}\right)^2} \tag{3}$$

It is expected that this damping is produced by the friction of linear sliders and thus the equivalent damping ratio can be estimated by Eq. (4).

$$h_{eq} \approx \frac{1}{4\pi}\left(\frac{\Delta W}{W}\right) \qquad \begin{cases} \Delta W = 4u_m Q_y \\ W = \frac{1}{2}\left(K_f u_m^{\,2} + Q_y u_m\right) \end{cases} \tag{4}$$

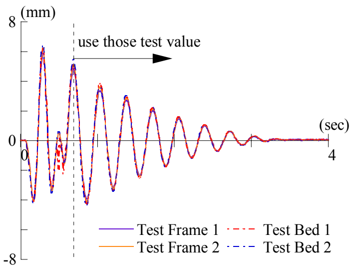

Figure 11 Acceleration Time History of Shaking Table

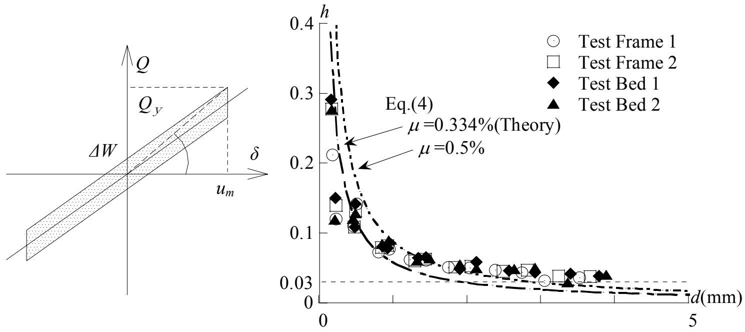

Figure 12 Equivalent Damping Ratios

Here, ΔW (shaded area in Figure 12) is one cycle energy produced by the friction force of linear sliders, and W, the potential energy of the test frame with an amplitude of u_m. The maximum friction force Q_y is obtained from the mass of the system multiplied by the dynamic friction coefficient μ obtained from Eq. (5).

$$\mu = 0.0028907 + 5.6114 \times 10^{-6} \times P \tag{5}$$

Estimating the mass as 62.5 ton and μ as 0.0033, Q_y becomes 2.03 kN and the horizontal stiffness of the test frame K_f becomes 22.2 kN/mm. The damping constant h obtained from those figures is shown in Figure 12.
The result shows that the damping ratio of the system is affected by the amplitudes; however, it converges to 0.03 when the amplitude becomes larger than 3 mm. Further, the test results are consistent with the theoretical values derived from Eq. (4).

3.2. BCJ-L2 LOADING TEST

Next, an artificial seismic wave of BCJ-L2 (A_{max} = 356 cm/sec^2), whose time axis is reduced by half, is applied to the system. The shear force measured by the load cell is compared with those derived from the strain gauges on the columns of the test frame, as shown in Figure 13. From this figure, the load cell system is confirmed to be sufficiently accurate to measure the shear force introduced into the layer. The relationship between the shear force and the displacement obtained by the test is shown in Figure 14, while the hysteretic curves of plastic split-tees 1 and 2 are shown in Figures 15 and 16, respectively. Plastic split-tee 1 fractured at the third wave of BCJ-L2, which is consistent with the expectation as per Eq. (2); however, until the fracture, the split-tee exhibited a stable hysteretic curve. A simple analytical model is developed to evaluate the test result. This analytical model is shown in Figure 17, and the member size of the model is shown in Table 1. The yield strength of each member is shown in the table, which is derived from the coupon tests. The mass of the test beds is divided equally in each node points, and the damping constant is set as the result of the sine wave loading test.

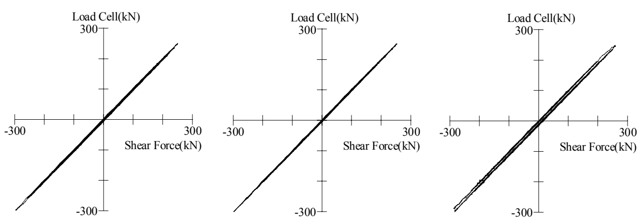

a) 1st b) 2nd c) 3rd

Figure 13 Load Comparison

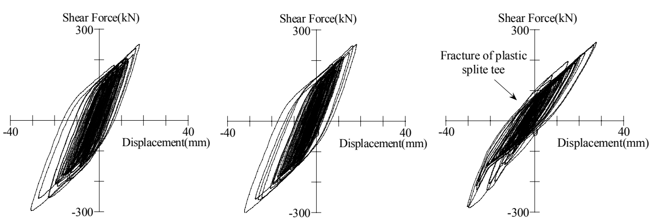

a) 1st b) 2nd c) 3rd

Figure 14 Shear Force-Displacement Relationships

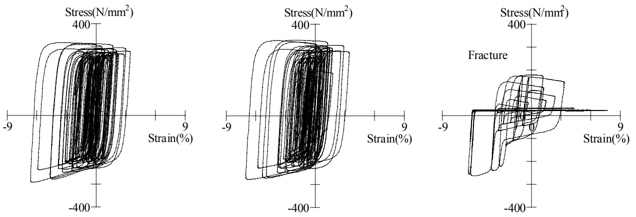

a) 1st b) 2nd c) 3rd

Figure 15 Hysteretic Curve of Plastic Split-Tee 1

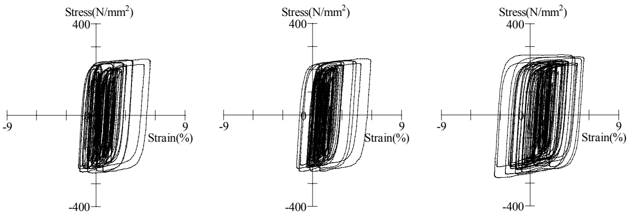

a) 1st b) 2nd c) 3rd

Figure 16 Hysteretic Curve of Plastic Split-Tee 2

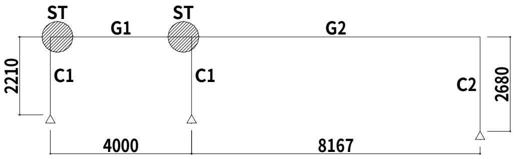

Figure 17 Analysis Model

Table 1 Member Characteristic

CODE	DIMENSION	STEEL PRODUCT	YIELD POINT(N/mm2)
C1	H-400×200×16×19	SS400	300
C2	H-200×200×9×19	SS400	300
G1	H-630×200×12×16	SS400	300
G2	H-450×200×9×9	SS400	300
ST	PL-60×12(Plastic Area100mm)	LY225	225

The response spectrum of the target earthquake wave is compared with that of the measured earthquake wave in the test, as shown in Figure 18. This figure shows that the response spectrum of the observed earthquake wave is larger than that of the target earthquake wave. However, in an elastic natural period, the response spectrum is generally consistent when the measured earthquake wave is used for analyses.

The time-histories of the displacement along the Y-direction obtained from the test and the analysis are compared in Figure 19. This figure shows that the test results and the analytical results are in good agreement, and the test bed system simulates the analytical results effectively.

The shear force and displacement relationship of the test frame is shown in Figure 20. From these figures, it is confirmed that the test results are generally consistent with the analytical results. In the test, the horizontal stiffness of the test frame before the fracture of the plastic split-tee is 22.2 kN/mm, which is almost the same as the value in the elastic loading test.

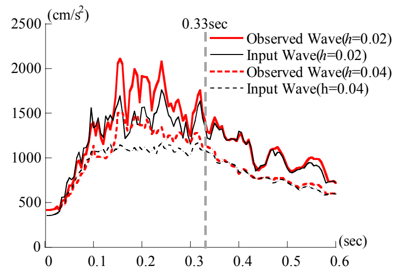

Figure 18 Response Spectrum

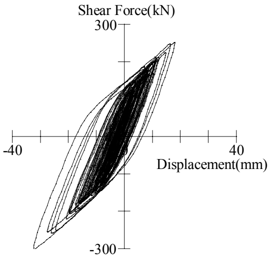

ii) Test Value

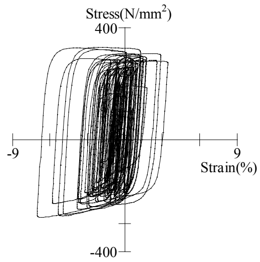

ii) Test Value

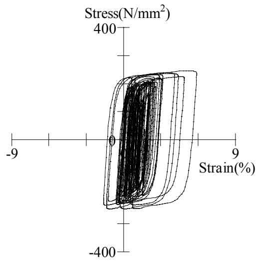

ii) Test Value

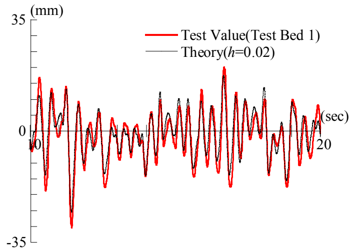

Figure 19 Displacement in Y-Direction

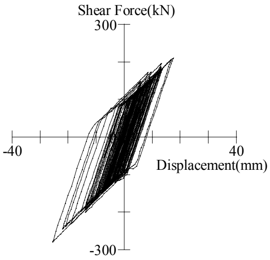

i) Analyses (h=0.02)

Figure 20 Shear Force-Displacement

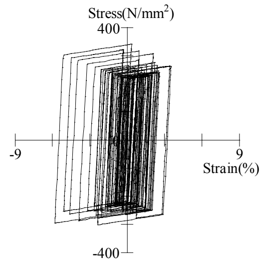

i) Analyses (h=0.02)

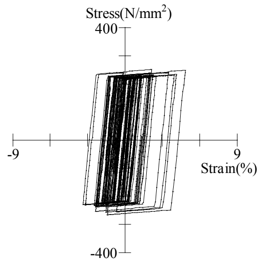

i) Analyses (h=0.02)

a) Plastic Split-Tee 1 b) Plastic Split-Tee 2

Figure 21 Hysteretic Curve of Plastic Split-Tee

In these studies, the horizontal stiffness of the test frame after the fracture of the plastic split-tee is reduced to 6.31 kN/mm. The hysteretic curves of the plastic split-tee obtained from the analyses are shown in Figure 21. These figures show that the response of the plastic split-tee in the test is also consistent with the analytical results.

3.3 JMA-KOBE LOADING TEST

After the fractured plastic split-tees were replaced, the same frame was applied to a JMA-KOBE earthquake wave (A_{max} = 818 cm/sec^2), whose time axis was reduced by half. A part of the results is shown in Figure 22. In the third cycle of the first earthquake, plastic split-tee 1 and the connecting bolts of elastic split-tee 2 fractured. However, the maximum response was consistent with the values expected from the analyses, and an effective response-reduction by the beam-end dampers was observed.

The response spectrum of the target earthquake wave is compared with that of the observed earthquake wave in Figure 23. This figure shows that the response spectrum of the measured earthquake wave is approximately 10% larger than that of the target earthquake wave hence the measured wave is used for the following analyses. The time-history of the axial force between the load cells around the fracture of the split-tees is shown in Figure 24. From this figure, it is observed that the axial force in the beam is decreased by 360 kN after the fracture of plastic split-tee 1 and the connecting bolts of elastic split-tee 2. This implies that the axial forces were initially introduced into the beam when replacing the plastic split-tees, and they were released at the fracture of the split-tees.

Next, the relationship between the shear force and the displacement along the Y-direction and the hysteretic curves of plastic split-tees 1 and 2 until fracture are shown in Figure 25. In these figures, the test results are compared with the analytical ones until fracture. This figure also shows that the test results are generally consistent with the analytical results. Further, the fracture point is roughly the same as that predicted by Eq. (2).

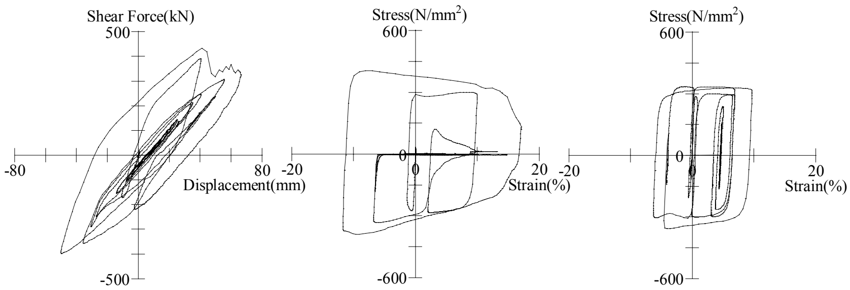

a) Load-Displacement b) Hysteresis Curve of Plastic Split-Tee 1 c) Hysteresis Curve of Plastic Split-Tee 2

Figure 22 Test Result input JMA-KOBE

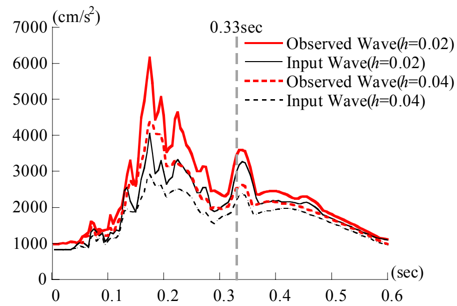

Figure 23 Response Spectrum

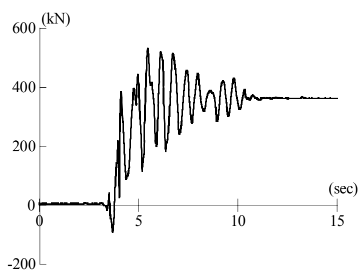

Figure 24 Axial Load in the Beam

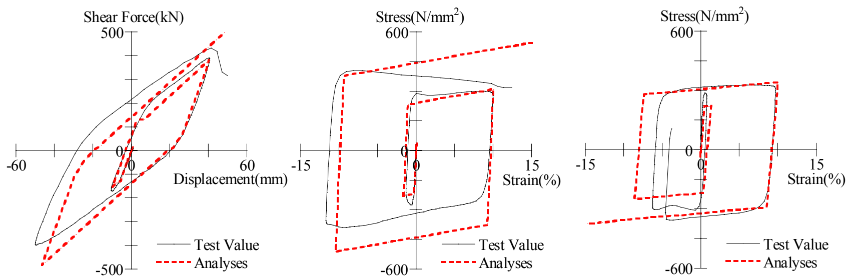

a) Load-Displacement b) Hysteresis Curve of Plastic Split-Tee 1 c) Hysteresis Curve of Plastic Split-Tee 2

Figure 25 Theory and Test Value Comparison

4. CONCLUSIONS

A multipurpose inertial mass system called "test bed" was constructed, and shaking table tests of a single-story test frame with beam-end dampers were conducted using this system. The following conclusions were obtained.

1) The dynamic characteristics of the setup system are consistent with the design values. The equivalent damping constant is derived from the friction force of the linear slider; it is less than 0.03 when the amplitude is larger than 3 mm.
2) It was confirmed that the shear force measured by the load cells corresponded to that delivered from the strain gauges on the test frame columns.
3) From the shaking table test using seismic waves, it was confirmed that the obtained response value was consistent with the analytical results.
4) Further, it was confirmed that the hysteretic curves and fracture points of plastic split-tees obtained by the test are consistent with the analytical evaluations.

From the above conclusions, the shaking table test using the constructed test bed system is considered to be effective for simulating the dynamic response of structural systems. Further experiments with multistory layers are under consideration.

ACKNOWLEDGEMENTS

This study is a part of "NEES/E-Defense collaborative research program on steel structures", and was pursued by the Test Bed and Innovative System Working Group (WG). The Japan team leader for the overall program is K. Kasai, and the WG leader is T. Takeuchi, both at Tokyo Institute of Technology. The writers acknowledge financial support provided by the National Research Institute for Earth Science and Disaster Prevention.

REFERENCE

Kasai, K., Takeuchi, T., Ooki, Y., Motoyui, S., Matsuoka, Y. (2007). E-Defense Tests on Full-Scale Steel Buildings, Part 1 - Experiments using Dampers and Isolators. ASCE Structural Congress 2007 (Long Beach), 247-17.

Takeuchi, T., Kasai, K., Midorikawa, M., Matsuoka, Y. (2007). E-Defense Tests on Full-Scale Steel Buildings, Part 4 - Multipurpose Test Bed for Efficient Experiments. ASCE Structural Congress 2007 (Long Beach), 247-20.

Kishiki, S., Yamada, S., Takeuchi, T., Suzuki, K., Wada, A. (2004). New Ductile Steel Frames Limiting Damage to Connection Elements at the Bottom Flange of Beam-Ends (Part.1). 7th Pacific Structural Steel Conference (PSSC 2004).

Takeuchi, T., Ida, M., Yamada, S., Suzuki, K. (2008). Estimation of Cumulative Deformation Capacity of Buckling Restrained Braces. Journal of Structural Eng., ASCE, 822-831, Vol. 134.

Takeuchi, T., Shirabe, H., Yamada, S., Kishiki, S., Suzuki, K., Saeki, E., Wada, A. (2006). Cumulative Deformation Capacity and Damage Evaluation for Elast-Plastic Dampers at Beam Ends. J. Struct. & Constr. Eng., A.I.J., No.600, 115-122.